

## Sawtooth Oscillation in Current-Carrying Plasma in the Large Helical Device

Y. Nagayama,<sup>1</sup> K. Kawahata,<sup>1</sup> S. Inagaki,<sup>1</sup> B. J. Peterson,<sup>1</sup> S. Sakakibara,<sup>1</sup> K. Tanaka,<sup>1</sup> T. Tokuzawa,<sup>1</sup> K. Y. Watanabe,<sup>1</sup> N. Ashikawa,<sup>1</sup> H. Chikaraishi,<sup>1</sup> M. Emoto,<sup>1</sup> H. Funaba,<sup>1</sup> M. Goto,<sup>1</sup> Y. Hamada,<sup>1</sup> K. Ichiguchi,<sup>1</sup> K. Ida,<sup>1</sup> H. Idei,<sup>1</sup> T. Ido,<sup>1</sup> K. Ikeda,<sup>1</sup> S. Imagawa,<sup>1</sup> A. Isayama,<sup>2</sup> M. Isobe,<sup>1</sup> A. Iwamoto,<sup>1</sup> O. Kaneko,<sup>1</sup> S. Kitagawa,<sup>1</sup> A. Komori,<sup>1</sup> S. Kubo,<sup>1</sup> R. Kumazawa,<sup>1</sup> S. Masuzaki,<sup>1</sup> K. Matsuoka,<sup>1</sup> T. Mito,<sup>1</sup> J. Miyazawa,<sup>1</sup> T. Morisaki,<sup>1</sup> S. Morita,<sup>1</sup> O. Motojima,<sup>1</sup> S. Murakami,<sup>1</sup> T. Mutoh,<sup>1</sup> S. Muto,<sup>1</sup> N. Nakajima,<sup>1</sup> Y. Nakamura,<sup>1</sup> H. Nakanishi,<sup>1</sup> K. Narihara,<sup>1</sup> Y. Narushima,<sup>1</sup> A. Nishimura,<sup>1</sup> K. Nishimura,<sup>1</sup> A. Nishizawa,<sup>1</sup> N. Noda,<sup>1</sup> S. Ohdachi,<sup>1</sup> K. Ohkubo,<sup>1</sup> N. Ohyabu,<sup>1</sup> Y. Oka,<sup>1</sup> M. Osakabe,<sup>1</sup> T. Ozaki,<sup>1</sup> A. Sagara,<sup>1</sup> K. Saito,<sup>1</sup> R. Sakamoto,<sup>1</sup> M. Sasao,<sup>1</sup> K. Sato,<sup>1</sup> T. Seki,<sup>1</sup> T. Shimozuma,<sup>1</sup> M. Shoji,<sup>1</sup> H. Suzuki,<sup>1</sup> S. Sudo,<sup>1</sup> K. Takahata,<sup>1</sup> Y. Takeiri,<sup>1</sup> K. Toi,<sup>1</sup> K. Tsumori,<sup>1</sup> H. Yamada,<sup>1</sup> I. Yamada,<sup>1</sup> K. Yamazaki,<sup>1</sup> N. Yanagi,<sup>1</sup> M. Yokoyama,<sup>1</sup> Y. Yoshimura,<sup>1</sup> Y. Yoshinuma,<sup>1</sup> T. Watari,<sup>1</sup> and LHD Group<sup>1</sup>

<sup>1</sup>National Institute for Fusion Science, Toki 509-5292, Japan

<sup>2</sup>Japan Atomic Energy Research Institute, Naka 311-0193, Japan

(Received 14 August 2002; published 20 May 2003)

Sawtooth oscillations have been observed in current-carrying helical plasmas by using electron-cyclotron-emission diagnostics in the Large Helical Device. The plasma current, which is driven by neutral beam injection, reduces the  $\beta$  threshold of the sawtooth oscillation. When the central  $q$  value is increased due to the plasma current, the core region crashes, and, when it is decreased, the edge region crashes annularly. Observed rapid mixture of the plasma in the limited region suggests that these sawtooth crashes are reconnection phenomena. Unlike previous experiments, no precursor oscillation has been observed.

DOI: 10.1103/PhysRevLett.90.205001

PACS numbers: 52.35.Py, 52.35.Vd, 52.55.Hc

Sawtooth oscillation is a series of periodic crashes, which is commonly observed magnetohydrodynamic (MHD) activity in tokamak plasmas [1], and it has been of interest to plasma physicists as an important example of the magnetic reconnection phenomena [2]. The sawtooth oscillation is usually accompanied with the collapse of the central region, which is called the full crash. The mechanism of sawtooth oscillation has been discussed for a long time. The well-known full reconnection model is as follows: the  $(m, n) = (1, 1)$  tearing mode drives the reconnection of field lines inside and outside of the  $q = 1$  surface and causes the fast parallel transport phenomena along the field line [3]. Here,  $m$  and  $n$  are the poloidal and the toroidal mode numbers, respectively. This model is consistent with the soft x-ray tomography measurement [4], but is not consistent with the observed crash time [5] or with the  $q$  profile measurement [6]. Considered three dimensionally, the full reconnection model implies that the set of reconnection points forms an  $m = 1$  helical line around the torus [7]. However, detailed observation of the sawtooth crash using electron-cyclotron-emission (ECE) diagnostics suggests that the reconnection occurs at a toroidally localized place [7]. This is called localized reconnection. Numerical simulation [8] shows that the ballooning mode causes the localized reconnection process in high  $\beta$  plasmas. Here,  $\beta$  is the ratio of the plasma pressure to the magnetic pressure of the external field.

Sawtooth oscillations are also observed in helical systems [9–11]. In helical systems, the kink, the tearing, and the ballooning modes should be stable, since the plasma current is very low and the shear is reversed [12,13]. So

sawtooth oscillations in a helical system should provide new information for MHD physics. It has been observed that the annular sawtooth crash takes place in helical plasmas, and the accompanied precursors are the  $(1, 1)$  mode [9], the  $(3, 2)$  mode [10] and the  $(2, 1)$  mode [11]. It has been considered that the sawtooth crash is caused by the reconnection driven by the low- $n$  interchange mode in a high-negative-shear helical system [14].

This Letter will present the sawtooth oscillation in the current-carrying helical plasma in the Large Helical Device (LHD): the largest superconducting heliotron-type fusion device with the averaged minor radius  $a = 0.65$  m, and the major radius of the plasma axis  $R_{ax} = 3.6$  m [15]. The plasma current is driven by the neutral beam injection (NBI), and the direction (co- or counter-) of the toroidal current can be controlled. Here, the co-current is defined as the current that raises the central  $\iota$ . The  $\iota$  is the rotational transform and is related to the  $q$  value as  $\iota/2\pi = 1/q$  [13]. In this work, the sawtooth is observed with the ECE [16,17] and the 12-channel far-infrared laser interferometer (FIR) diagnostics [18]. Using ECE diagnostics, the sawtooth crash can be observed with higher spatial resolution than the previous experiments. A significant observation in this work is that the full sawtooth crash with an interchange phenomenon takes place when the plasma current flows in the counter-direction, and that the annular crash without precursor takes place when the current flows in the codirection in LHD. In both cases, evidence of reconnection has been observed. Results shown in this Letter give a new perspective to sawtooth physics.

Figure 1 shows the heating power, the plasma current, the  $\beta$ , the line averaged electron density ( $\langle n_e \rangle$ ), and the ECE signals during the sawtooth oscillation in the helical plasma with counter-current in LHD. The plasma current is measured with Rogowskii coils, which are installed both inside and outside of the vacuum vessel wall. By compensating the stray field, the  $\beta$  is obtained from the toroidal flux, which is measured by a poloidal loop on the inner surface of the vacuum vessel.  $\langle n_e \rangle$  is defined as the line integrated density divided by the chord length, which is the length of the viewing line inside the flux surface of  $\rho = 1.1$ , where  $n_e$  vanishes in LHD. The plasma with  $B_{ax} = 2.75$  T and  $R_{ax} = 3.6$  m is heated by the counter-beam with a deposited power of 5.4 MW and by the ECH with a frequency of 168 GHz and a power of 0.7 MW. The solid line indicates the plasma with the sawtooth oscillation (#33734), and the broken line indicates the plasma without the sawtooth oscillation (#33730). The plasma confinement is slightly degraded due to the sawtooth oscillation.

Figures 2(a) and 2(b) show contour plots of the time evolution of the electron temperature ( $T_e$ ) profile and of the  $\Delta T_e$  on the midplane, respectively. Here, the  $\Delta T_e$  is defined as  $\Delta T_e = T_e - [T_e]_{\min}$ , where  $[T_e]_{\min}$  is the mini-

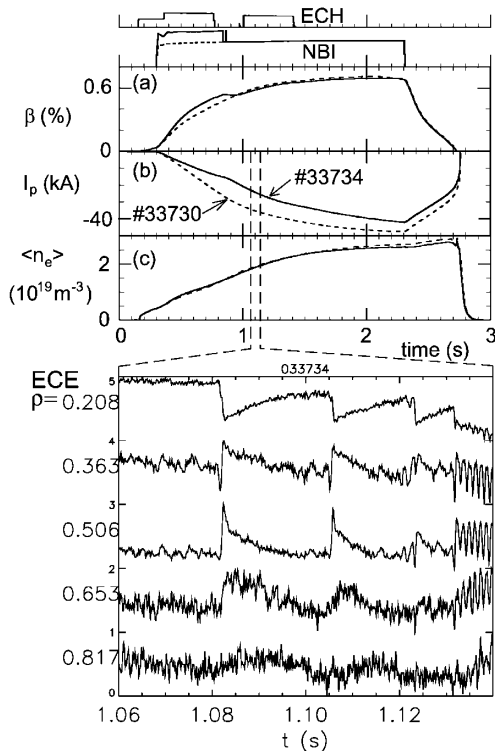


FIG. 1. Heating and plasma parameters in a counter-NBI heated LHD plasma with sawtooth oscillation: (a) plasma  $\beta$ ; (b) plasma current ( $I_p$ ); (c) line averaged electron density; (d) ECE signals. The solid line indicates the plasma with the sawtooth oscillation (#33734), and the broken line indicates the plasma without the sawtooth oscillation (#33730).

um over the full time interval of the sawtooth period. The  $T_e$  profile is measured with the 32-channel radiometer [17] covering  $R_{ax} = 2.9$ – $3.5$  m. The radiometer data are cross calibrated to the Michelson interferometer [16]. The contour plot of  $\Delta T_e$  provides a visual presentation of the heat transfer during the sawtooth crash process. Before the sawtooth crash, the  $\Delta T_e$  is concentrated in the core region, and, after the crash, the  $\Delta T_e$  is localized in the region between the inversion surface and the mixing surface, as shown in Figs. 2(b) and 3(a). Therefore, the electron thermal energy transfers from the inside to the outside of the inversion surface during the sawtooth crash process. The wave form of the ECE signal [Fig. 1(c)] and the behavior of the contour plots of  $\Delta T_e$  are similar to those of the sawtooth crash in tokamak plasmas [7]. Therefore, the magnetic reconnection may play an important role.

The mixing surface ( $\rho = 0.58$ ) is close to the  $\iota/2\pi = 1/2$  surface ( $\rho = 0.55$ ). The sinusoidal oscillation superimposes on the later phase of the sawtooth oscillation as shown in Fig. 1 ( $t = 1.12$  s). Finally this oscillation becomes dominant and the sawtooth oscillation disappears. The mode numbers of the sinusoidal oscillation are determined as (3,1) and/or (2,1) from the mode analysis of

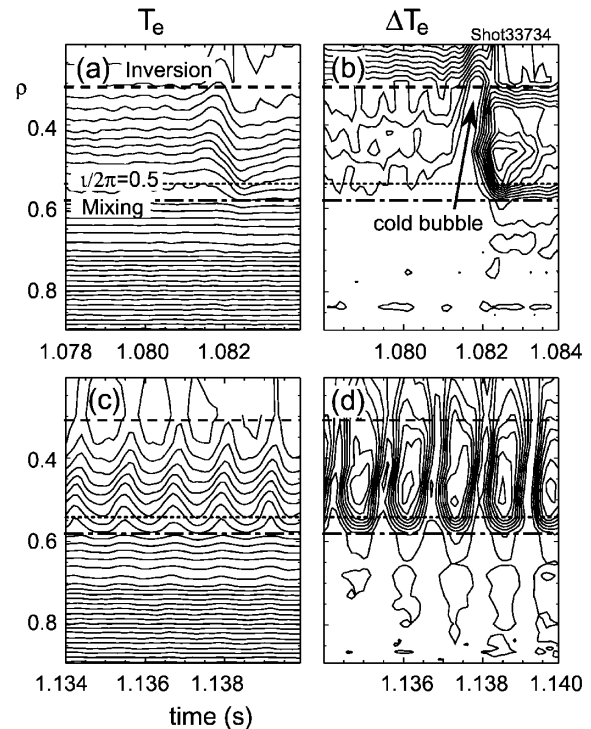


FIG. 2. (a) Time evolution of electron temperature ( $T_e$ ) profile and (b) contour plot of time evolution of  $\Delta T_e$  during the sawtooth crash in the counter-NBI heated LHD plasma. (c) Contour plot of time evolution of the  $T_e$  profile and (d) contour plot of time evolution of  $\Delta T_e$  during the sinusoidal MHD activity. The contour step size is 50 and 15 eV in the  $T_e$  and the  $\Delta T_e$  profiles, respectively.

Mirnov signals. Since the sinusoidal oscillation has the period of 5 ms and the plasma rotates toroidally, the frequency of plasma rotation is 0.2 kHz. Figures 2(c) and 2(d) show contour plots of the time evolution of the  $T_e$  profile and of the  $\Delta T_e$  during the sinusoidal oscillation, respectively. The main part of this MHD activity is located inside the mixing surface, which is close to the  $\iota/2\pi = 0.5$  surface. No heat transfer from the core region to the peripheral region is observed due to the sinusoidal oscillation, so the sinusoidal oscillation does not accompany the magnetic island structure. The sinusoidal oscillation is not related to the sawtooth but the unstable condition may be close to that of the sawtooth oscillation. A precursor oscillation for the full crash has not been observed. As the crash time of  $\sim 1$  ms is much shorter than the period of plasma rotation, we cannot know whether a precursor does or does not exist.

Figures 4(a)–4(c) show the heating,  $\langle n_e \rangle$ , the plasma current ( $I_p$ ), and the  $\beta$  in the plasma with the sawtooth oscillation and with the cocurrent. The plasma has  $B_{ax} = 2.8$  T and  $R_{ax} = 3.6$  m, and it is heated by the cobeam with the deposited power of 6.2 MW. The sawtooth oscillation appears on the  $\beta$  signal. The ECE at  $\rho = 0.73$  drops and the ECE at  $\rho = 0.89$  increases at  $t = 1.76$  s. As shown in Figs. 3(c) and 3(d), the normalized inversion radius is about  $\rho = 0.85$ , where the  $\iota/2\pi$  is nearly 1. The ECE in the region between  $\rho = 0.7$  and  $\rho = 0.85$  drops, and the ECE in the region of  $\rho > 0.85$  increases at  $t = 1.76$  s. This is an annular crash. The decrease of the ECE in the region of  $\rho < 0.7$  delays as the ECE position departs from the inversion radius. So the cold pulse propagates in the inward direction.

Since  $\langle n_e \rangle$  drops at  $\rho = 0.9$  and increases at  $\rho = 1.09$  during the crash, the inversion of  $\langle n_e \rangle$  is between  $\rho = 0.9$  and  $\rho = 1.09$ . Thus, the inversion radius of  $n_e$  is larger than that of  $T_e$ . A simple interpretation of these phenomena is that the density crash and the temperature crash each take place at a different place. Another interpretation is as follows: The reconnection mixes plasma near the inversion surface simultaneously. The mixing region is between the inner and the outer mixing surfaces in the case of the annular crash. If the  $T_e$  profile is peaked and the  $n_e$  profile is very flat, the difference between the inversion radii of  $T_e$  and  $n_e$  can be explained.

Figure 4(k) shows the Mirnov signals in the fast time scale. In the Mirnov signal, a steady mode with the frequency of  $\sim 7$  kHz is observed before the crash. Although Mirnov signal is enhanced during the crash, the frequency and the mode number do not change. The mode numbers are  $m = 4 \pm 1$  and  $n = 5 \pm 1$ , so the plasma rotates steadily with the frequency of  $\sim 1.4$  kHz. Figures 4(d), 4(e), and 4(h)–4(j) show the ECE and  $\langle n_e \rangle$  signals in the fast time scale. No precursor oscillation has been observed in the ECE,  $\langle n_e \rangle$ , or Mirnov signals.

Figure 5 shows trajectories of LHD discharge with high plasma current in the space of the plasma current vs  $\beta$ .

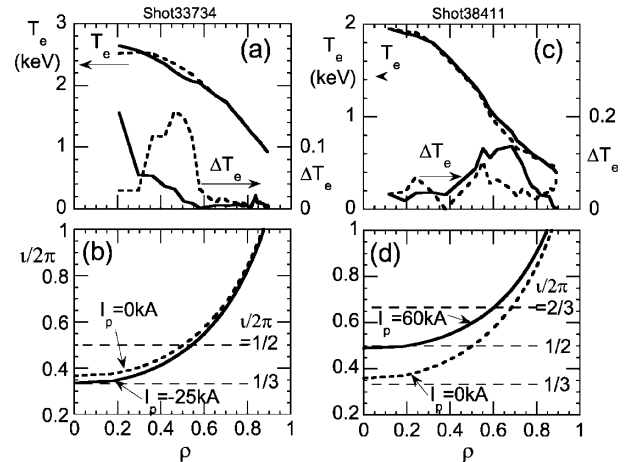


FIG. 3. (a)  $T_e$  profile before (broken line) and after (solid line) the sawtooth crash in the LHD plasma with counter-current. (b) Calculated  $\iota/2\pi$  profile with (solid line) and without (broken line) the plasma current in the counterdirection. (c)  $T_e$  profile before (broken line) and after (solid line) the sawtooth crash in the LHD plasma with cocurrent. (d) Calculated  $\iota/2\pi$  profile with (solid line) and without (broken line) the plasma current in the codirection.

These data are obtained in the beam heated plasmas with  $R_{ax} = 3.6$  m and  $B_{ax} = 2.75$ –2.8 T. Sawtooth oscillation is observed on the region indicated by thick lines, and is not observed on dotted lines in Fig. 5. In the case of low plasma current, the sawtooth has not been observed in the plasma with a flat density profile, but is observed in the plasma with the peaked density profile when  $\beta$  is nearly 1% [19]. Here low plasma current is defined as  $|I_p/B_{ax}| < 4$  kA/T. The  $\beta$  threshold of the sawtooth is reduced drastically due to the plasma current.

The  $\iota$  profiles considering the plasma current are shown in Figs. 3(b) and 3(d). These profiles are calculated using the three-dimensional equilibrium code VMEC [20] under the assumption of a parabolic current profile. In the case of counter-current, the  $\iota/2\pi$  in the sawtooth region is flat and is very close to 1/3. As shown in Fig. 2(b), a cold plasma comes into the core region from the region between the inversion and the mixing radii. This is an interchange process, and it is similar to Wesson's quasi-interchange model that the kink mode draws a cold bubble into the core region and causes the sawtooth crash when the  $q$  profile is very flat in the core region [21]. In the helical system, the interchange mode has been considered to play an important role in the sawtooth crash [14]. A speculation on the role of cocurrent is as follows: The cocurrent reduces the radius of the  $\iota/2\pi = 1$  surface so that the pressure gradient at the rational (cf.  $\iota/2\pi = 1$ ) surface increases. Finally a pressure driven mode becomes unstable and it drives a reconnection due to some resistivity.

In summary, by using the ECE diagnostics, we have discovered new types of sawtooth crashes in helical

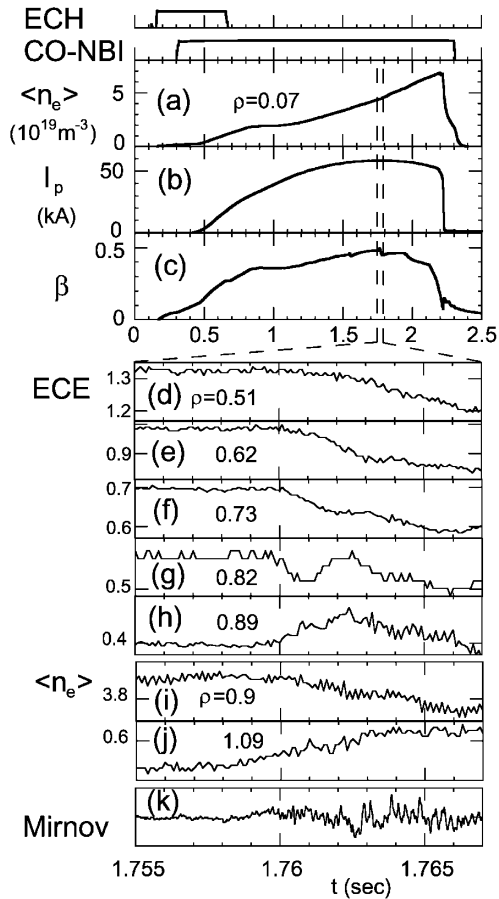


FIG. 4. Heating and plasma parameters in the co-NBI heated LHD plasma. (a) The line average electron density ( $\langle n_e \rangle$ ) at the chord of  $\rho = 0.07$ , (b) plasma current ( $I_p$ ), (c) plasma  $\beta$  in the slow time scale. (d)–(h) ECE signals; (i)–(j)  $\langle n_e \rangle$  in the edge region; (k) Mirnov coil signal in the fast time scale.

plasmas in LHD: one is the full sawtooth crash in the case of counter-current, and another is the annular crash in the case of co-current. The plasma confinement is slightly degraded due to the sawtooth oscillation. An observed rapid mixture of the plasma in the limited region suggests that sawtooth crashes in LHD are reconnection phenomena. Outward heat pulse propagation in the case of a full crash and the inward cold pulse propagation in the case of an annular crash have been observed. The plasma current reduces the  $\beta$  threshold of the sawtooth oscillation. In the calculation, the counter-current makes the  $\nu$  profile flat with  $\nu/2\pi \sim 1/3$  in the core region. Interestingly, the interchange phenomenon has been observed in the case of a full crash. So, the full crash may be driven by the interchange mode in LHD, but the observed  $m = 3$  or  $m = 2$  modes do not cause the crash. In the case of the annular crash, the plasma rotation is fast enough to observe a low  $n$  mode but no precursor has been observed. The localized mode may cause the annular crash, but in

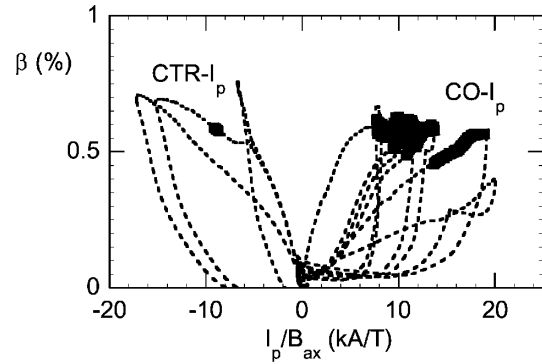


FIG. 5. Trajectories of LHD plasma in a space of plasma current vs  $\beta$ . Thick line indicates the region where the sawtooth oscillations is observed.

the present theory the ballooning mode is usually stable due to the reversed shear in LHD. The driving instability of the sawtooth crash has not been identified in LHD. Further theoretical and experimental works are needed to understand the sawtooth oscillation in the helical system.

- [1] S. von Goeler, W. Stodiek, and N. Sauthoff, Phys. Rev. Lett. **33**, 1201 (1974).
- [2] M. Yamada *et al.*, Phys. Plasmas **1**, 3269 (1994).
- [3] B. B. Kadomtsev, Sov. J. Plasma Phys. **2**, 533 (1976).
- [4] C. Janicki, R. Decoste, and C. Simm, Phys. Rev. Lett. **62**, 3038 (1989).
- [5] A. W. Edwards *et al.*, Phys. Rev. Lett. **57**, 210 (1986).
- [6] H. Soltwisch, Rev. Sci. Instrum. **59**, 1599 (1988).
- [7] Y. Nagayama *et al.*, Phys. Plasmas **3**, 1647 (1996).
- [8] Y. Nishimura, J. D. Callen, and C. C. Hegna, Phys. Plasmas **6**, 4685 (1999).
- [9] J. H. Harris *et al.*, Phys. Rev. Lett. **53**, 2242 (1984).
- [10] H. Zushi *et al.*, Nucl. Fusion **27**, 895 (1987).
- [11] S. Takagi *et al.*, Rev. Sci. Instrum. **72**, 721 (2001).
- [12] V. D. Shafranov, Phys. Fluids (1958–1988) **26**, 357 (1983).
- [13] J. P. Freidberg, *Ideal Magnetohydrodynamics* (Plenum Press, New York, 1987).
- [14] M. Wakatani, H. Shirai, and M. Yamagiwa, Nucl. Fusion **24**, 1407 (1984).
- [15] M. Fujiwara *et al.*, Nucl. Fusion **41**, 1355 (2001).
- [16] Y. Nagayama *et al.*, Fusion Eng. Des. **53**, 201 (2001).
- [17] K. Kawahata *et al.*, Rev. Sci. Instrum. (to be published).
- [18] K. Kawahata *et al.*, Rev. Sci. Instrum. **70**, 707 (1999).
- [19] S. Ohdachi *et al.*, in Proceedings of the 13th Stellarator Workshop, Canberra, 2002.
- [20] S. P. Hirshman and D. K. Lee, Comput. Phys. Commun. **39**, 143 (1986).
- [21] Wesson *et al.*, in *Plasma Physics and Controlled Nuclear Fusion Research: Proceedings of the 11th International Conference, Kyoto, 1986* (IAEA, Vienna, 1987), Vol. 2, p. 3.